Laser Excitation of Lattice-Driven Anharmonic Magnetization Dynamics in Dielectric $FeBO_3$

D. Afanasiev,[1,*] I. Razdolski,[1] K. M. Skibinsky,[2] D. Bolotin,[2] S. V. Yagupov,[2] M. B. Strugatsky,[2] A. Kirilyuk,[1] Th. Rasing,[1] and A. V. Kimel[1]

[1]*Radboud University Nijmegen, Institute for Molecules and Materials, 6525 AJ Nijmegen, The Netherlands*

[2]*Solid-State Physics Chair, Department of Physics, Taurida National University, 95036 Simferopol, Ukraine*

(Received 15 November 2013; published 9 April 2014)

Femtosecond laser pulses trigger in dielectric $FeBO_3$ coherent oscillations of the magnetic anisotropy followed by spins. The oscillations are driven by optically excited lattice vibrations strongly coupled to the magnetic system. Unlike the spin resonances, this mode is characterized by a very small damping ratio and can be easily pushed into an anharmonic regime.

DOI: 10.1103/PhysRevLett.112.147403 PACS numbers: 78.20.hc, 75.78.Jp, 78.20.Ls, 78.47.J-

Efficient control of spin dynamics by femtosecond (fs) laser pulses is a heavily debated topic in modern magnetism [1–4]. Such a control of spins is counterintuitive, since an action of the electric field of light on elementary electric dipoles, which is the strongest perturbation in light-matter interaction, conserves the spin of the electron [2]. Nevertheless, it was shown that excitation of metals or semiconductors with the help of a fs laser pulse can lead to a collapse of the magnetic order [5,6] or even magnetization reversal [7]. A crucial role in these phenomena is played by the free electron gas. The laser pulse heats the free electrons creating strongly nonequilibrium distribution, which eventually promotes the demagnetization and remagnetization of the metallic magnet [8]. Unfortunately, such a mechanism can hardly be realized in dielectric magnetic media where no free electrons are present. This obstacle has motivated an intense search for alternative ways to excite spin dynamics in magnetic dielectrics by means of light. Several mechanisms based on impulsive stimulated Raman scattering by magnons [9], photoinduced magnetic anisotropy [10], and resonant THz pumping [11] have been successfully demonstrated. Nevertheless, in all these approaches the amplitude of the excited spin dynamics was so small that the dynamics did not even enter an anharmonic regime.

Recently, an alternative way to control spins by light via coherent phonon excitation has been demonstrated in metals [12–14] and semiconductors [15]. Even a scenario of laser-induced acoustically mediated magnetization reversal was suggested theoretically [16]. All these articles reveal the potential of the coupled magnetoacoustic (MA) excitations for optical control of magnetism in dielectrics. Here we report that excitation of $FeBO_3$ by a fs laser pulse generates a standing acoustic wave. Because of a strong magnetoelastic coupling this excitation leads to coherent oscillations of the magnetic anisotropy followed by spins. Unlike the spin resonances, this mode is characterized by a very small damping and the efficiency of the excitation is high enough to push the spin dynamics into an anharmonic regime.

To demonstrate the laser-induced acoustically mediated magnetization dynamics in a dielectric medium we have chosen single-crystalline $FeBO_3$ (point group is D_{3d}^6). This is an antiferromagnet ($T_N = 348$ K) with strong anisotropy of an easy-plane type [17]. The magnetizations of the two antiferromagnetically coupled sublattices $\mathbf{M}_1$, $\mathbf{M}_2$ lie in the plane perpendicular to the C_3 crystallographic axis. The antisymmetric exchange leads to a canting of the sublattice magnetizations resulting in a net magnetic moment $\mathrm{M} = |\mathbf{M}_1 + \mathbf{M}_2| \approx 9$ emu/cm^3, also perpendicular to the C_3 axis. Because of the extremely low value of the intrinsic in-plane magnetic anisotropy $\mathrm{H_a} = 0.26$ Oe [18] iron borate is almost isotropic in the easy plane. It makes the spins highly susceptible to external perturbations, including stress [19] and light [20,21]. Moreover, iron borate has an extremely large value of the magnetoelastic contribution ΔC to the effective elastic modulus $C_{\mathrm{eff}} = C + \Delta C$ which in zero magnetic field could reach values up to $|\Delta C/C| = 0.8$ [22].

We studied a series of iron borate single crystals with thicknesses of 4 to 40 μm. All crystals had their crystallographic axis C_3 normal to the sample plane. Optical control of the magnetic anisotropy in $FeBO_3$ was studied with the help of a pump-probe technique with a mechanical delay line in the geometry shown in Fig. 1(a). We employed an amplified Ti:sapphire laser system producing 200 fs pulses with a central photon energy of 1.55 eV at a repetition rate of 1 kHz. The laser-induced magnetization dynamics was monitored measuring Faraday rotation $\theta_F = \chi(\mathbf{M}, \mathbf{e_k})$. Here, χ is the magneto-optical (MO) susceptibility and $\mathbf{e_k}$ is the unit vector in the direction of the light propagation. The intensity ratio between the pump and probe pulses was about 50. Both beams were focused on the sample to a spot diameter of about 200 μm for the pump and 60 μm for the probe. To avoid an influence of possible artifacts of nonmagnetic origin we measured polarization rotation θ at

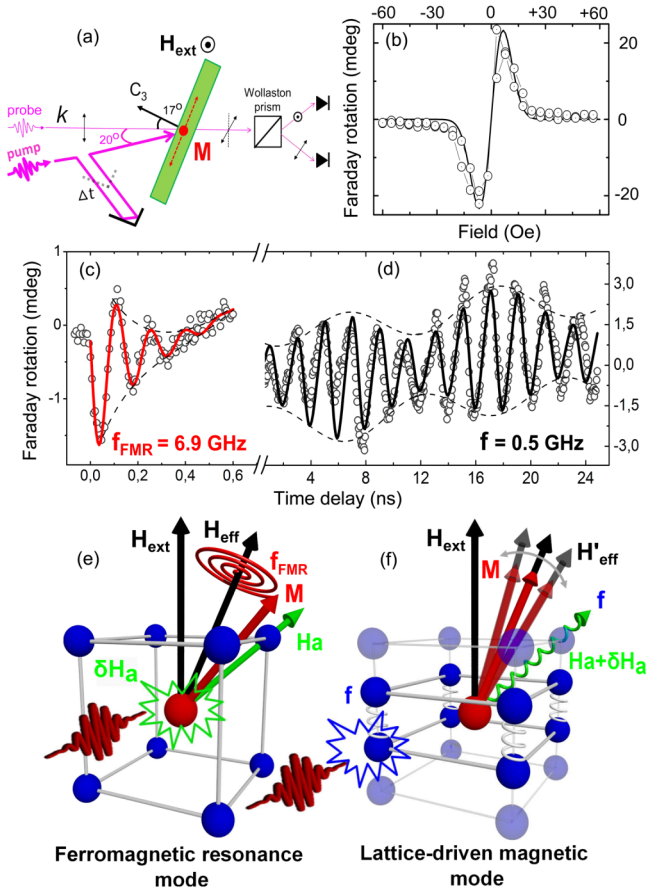

FIG. 1 (color online). (a) Experimental geometry of the optical pump-probe setup. (b) Static Faraday rotation in $FeBO_3$ as a function of in-plane external magnetic field. (c) Femtosecond laser excitation of short-living high frequency FMR mode at $f_{FMR} = 6.9$ GHz. (d) Femtosecond laser excitation of the long-living lattice-driven magnetic mode at $f = 0.5$ GHz. The external magnetic field is 40 Oe and the pump fluence is 38 mJ/cm^2. The sample thickness is 9 μm. (e) Schematic representation of light-induced FMR. Instantaneously induced magnetic anisotropy $\delta\mathbf{H_a}$ causes the magnetization $\mathbf{M}$ deviation from equilibrium followed by the precession around the effective magnetic fields $\mathbf{H_{eff}} = \mathbf{H_{ext}} + \mathbf{H_a}$. (f) Schematic representation of light-induced lattice-mediated oscillations of magnetic anisotropy. Ultrafast excitation of lattice induces periodic tensile and compression of the primitive cell, which generates a periodically modulated magnetic anisotropy $\delta\mathbf{H_a}$ and leads to a change of the equilibrium $\mathbf{H'_{eff}} = \mathbf{H_{ext}} + \mathbf{H_a} + \delta\mathbf{H_a}$. In the present picture $f \ll f_{FMR}$. For simplicity a bcc primitive cell with a magnetic atom (red) inside is chosen.

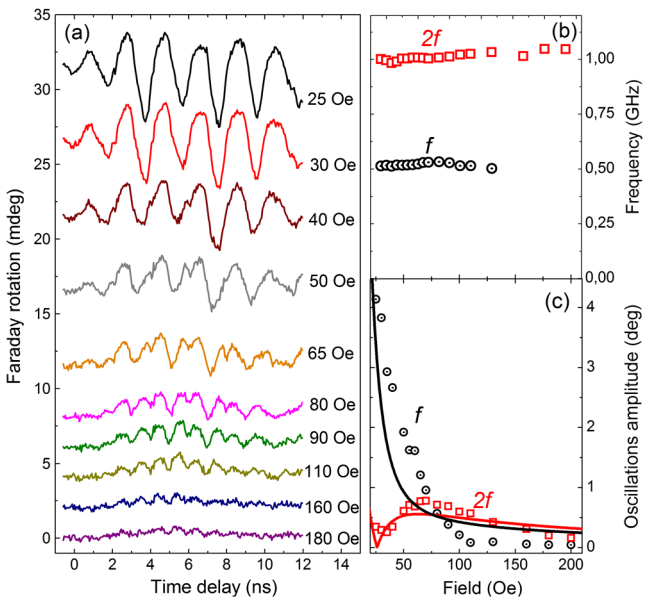

FIG. 2 (color online). (a) Probe polarization rotation as a function of time delay between linearly polarized pump and probe pulses for different values of the applied magnetic field. (b) Field dependence of frequencies of two harmonics. (c) Experimental data (points) and theoretical fit based on the theory (solid lines) of the amplitudes of the 1st and the 2nd harmonics of spin oscillations as a function of magnetic field. Fit parameters are $G_4 = 4.3 \times 10^7$ erg/cm^3 and $G_6 = 5.7 \times 10^4$ erg/cm^3, and the laser-induced strain amplitude is $s^0_{zz} = 3.3 \times 10^{-4}$. Sample thickness is 9 μm. Pump fluence is 38 mJ/cm^2.

two polarities of the external magnetic field $\mathbf{H_{ext}}$. The Faraday rotation then was calculated as the difference: $\theta_F = \frac{1}{2}[\theta(H^+_{ext}) - \theta(H^-_{ext})]$. The field $H_{ext} > 15$ Oe was applied in the sample plane ($\mathbf{H_{ext}} \perp \mathbf{e_k}$). Because of the weak in-plane anisotropy, the magnetization got oriented nearly along $\mathbf{H_{ext}}$, which was confirmed by static MO measurements [Fig. 1(b)]. All the measurements were done at room temperature.

Figure 1(c) shows that, similarly to Ref. [23], fs laser pulse excites strongly damped oscillations (the damping ratio is 0.16) at the frequency of the quasiferromagnetic resonance mode (FMR) $f_{FMR} = 6.9$ GHz. The dynamics at longer time delays reveals an additional low frequency 0.5 GHz, nearly damping-free oscillation (the damping ratio is ≤ 0.01) [Fig. 1(d)]. Figure 2(a) shows the low frequency oscillations in various external magnetic fields. It is remarkable that relatively small fields suppress the oscillations dramatically. A Fourier analysis of the signals spectra demonstrates both first f and second $2f$ harmonics of the magnetic excitation, with frequencies of 0.51 ± 0.05 and 1.01 ± 0.05 GHz, respectively. Both frequencies are hardly sensitive to the field strength [Fig. 2(b)]. This is in contrast to the behavior expected for the homogeneous magnetization precession around the effective magnetic field $\mathbf{H_{eff}}$ in $FeBO_3$; see Fig. 1(e). Moreover, observed frequencies are much lower than the FMR frequencies in $FeBO_3$. Hence, the observed magnetization oscillations cannot be due to a precession of the magnetization around its equilibrium orientation and can only be explained in terms of oscillations of the equilibrium orientation itself. As $f \ll f_{FMR}$, the magnetization tracks the equilibrium quasistatically. The oscillations of $\mathbf{H_{eff}}$ are due to oscillations of the laser-induced contribution to the anisotropy field

$\delta\mathbf{H_a}$, presumably triggered via the aforementioned lattice-driven effect [Fig. 1(f)].

To verify this hypothesis we performed the measurements on the samples of various thicknesses. The FMR frequency is expected to be thickness independent. Figure 3(a) shows that the thickness d strongly influences the frequency of the oscillations, while the amplitudes of the oscillations in all the samples are comparable, being in the range of 5–7 degrees. The thickness dependence of the lowest frequency f in the spectrum can be well described by $f = V_S/2d$, with $V_S = 8.7 \pm 0.1$ km/s [Fig. 3(b)]. This value is in a very good agreement with the speed of the longitudinal sound wave propagating along the C_3 axis [24]. It suggests that the observed oscillations of the magnetic anisotropy are due to a coupling between the magnetic subsystem and a laser-excited longitudinal sound wave. After the excitation such a wave is spatially confined by the sample surfaces. The boundary conditions given by the free surfaces lead, similarly to Ref. [25], to the formation of standing wave oscillating at the frequency f and described by the strain tensor component $s_{zz} = (\partial u/\partial z)$. Here $u(z)$ is a displacement of the atoms along $z \| C_3$. Such a standing strain wave results in periodic sample deformations along the z axis leading, in particular, to modulation of the volumetric mass density. In accordance with the Clausius-Mosotti relations it results in a change of the differential transmission [26] $\Delta T/T \sim 10^{-4}$ [Fig. 3(c)] and corresponds to a mechanical strain of $\sim 10^{-4}$. The frequencies of the oscillations in $\Delta T/T$ and the Faraday rotation are the same and field independent [Fig. 3(d)], but the amplitude of the oscillations in $\Delta T/T$ does not depend on the field.

To reveal the nature of the anharmonicity of the dynamics, we performed measurements for different pump fluences. Figures 4(a) and 4(b) show that the spectrum contains three harmonics effectively generated above the fluence threshold (20 mJ/cm^2). Note that the measured signal is proportional to the integral magnetization over the sample thickness. Hence, assuming a linear relationship between the strain and the magnetization [27], the odd harmonics can originate from the overtones of the acoustic standing wave. The even harmonics must have a different origin, because their integral effect over an integer number of periods is zero [25]. Indeed, Fig. 4(c) reveals nearly similar intensity dependencies for the 1st and 3rd harmonics, that are clearly distinct from that of the 2nd harmonic. Until the saturation near 44 mJ/cm^2, the 1st and 3rd harmonics have nearly linear dependence while the 2nd demonstrates a quadratic behavior. This implies that the 2nd harmonic arises from a nonlinear coupling between the magnetization and the sound. The different nature of the 1st and 2nd harmonics is also confirmed by their significantly different field dependencies [Fig. 2(c)]. In agreement with

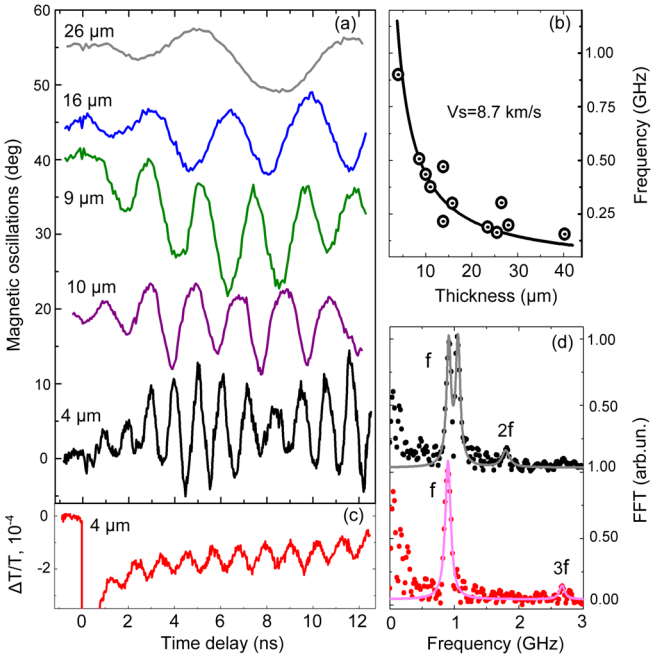

FIG. 3 (color online). (a) Magnetization deviation as a function of time for samples with various thicknesses. (b) Lowest frequency in the spectrum vs sample thickness: dots are experimental data, thick line is a hyperbolic fit $f = V_S/2d$. (c) Differential transmission signal for the sample with the thickness of 4 μm. (e) Normalized FFT spectra of the Faraday rotation (black) and the differential transmission (red) for a 4 μm thick sample. Solid lines are Lorentzian fits. The external field is 25 Oe. Pump fluence is 38 mJ/cm^2. The origin of the splitting of the f line in the FFT spectrum for the Faraday rotation could be due to a nonlinearity of the magnetoacoustic interation and an inhomogeneity of the sample thickness over the probed area.

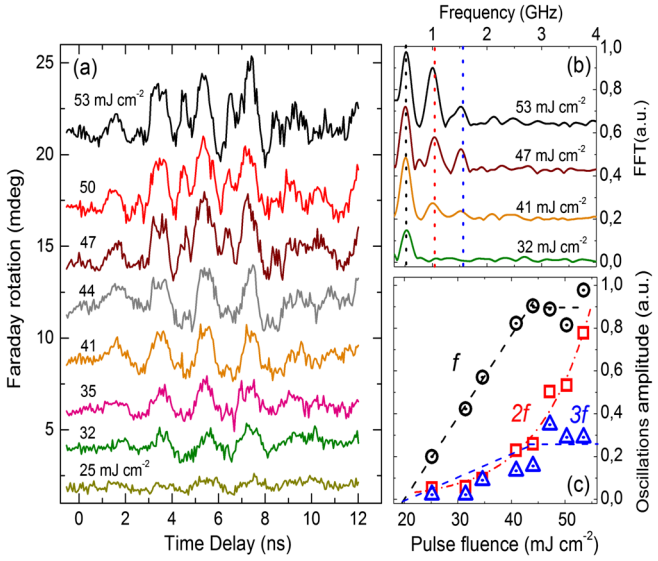

FIG. 4 (color online). (a) Probe polarization rotation as a function of time delay between the linearly polarized pump and probe pulses for different values of pump fluence. (b) FFT spectrum for different pump fluences. (c) Pump fluence dependence of the observed harmonics. The dashed lines are guides to the eye. External magnetic field is 100 Oe. Sample thickness is 9 μm.

this interpretation, our experiments show no 2nd harmonic in $\Delta T/T$ [see Fig. 3(d)].

We note that for $FeBO_3$, absorption of light at the pump wavelength is less than 80 cm^{-1}. Hence, it is reasonable to consider nondissipative mechanisms of the strain generation. Consider a coordinate system with the x and y axes in the plane of the sample and the z axis aligned along the C_3 axis. For the light incident close to the sample normal, the electric field is given by a superposition of x and y components $\mathbf{E} = E_x\mathbf{e}_x + E_y\mathbf{e}_y$, where $\mathbf{e}_x$ and $\mathbf{e}_y$ are unit vectors parallel to the x and y axes, respectively. The mechanical strain along the z axis can be generated by an electric field in a centrosymmetric crystal by means of an electrostrictionlike effect [28]: $s_{zz}(f) = \zeta_{zzxx}\mathrm{E}_x(\omega_1)\mathrm{E}_x*(\omega_2) + \zeta_{zzyy}\mathrm{E}_y(\omega_1)\mathrm{E}y^*(\omega_2) + \mathrm{c.c.}$, where ζ_{zzxx}, ζ_{zzyy} are components of the electrostriction tensor ζ_{ijkl} (for the space group of $FeBO_3$ $\zeta_{zzxx} = \zeta_{zzyy}$) and ω_1, ω_2 are the frequencies of the optical waves exciting the strain, so that $f = (\omega_1\text{-}\omega_2)/2\pi$. It is seen that the light-sound coupling does not depend on the orientation of the linear polarization of light. This has been confirmed experimentally. An ultrashot laser pulse is spectrally broad and simultaneously provides electric fields $\mathbf{E}(\omega_1)$ and $\mathbf{E}(\omega_2)$. Such a nondissipative mechanism can be explained in terms of impulsive stimulated Brillouin or Raman scattering [29,30].

For the space group of $FeBO_3$, a longitudinal sound wave along the C_3 axis can change neither the symmetry nor the direction of the magnetocrystalline anisotropy in the basal plane. Instead, it can trigger oscillations of its value [31]. This may happen due to strain-induced changes in the dipole-dipole and the single-ion magnetic interactions [32]. If the easy axis does not coincide with the external field, such oscillations will lead to oscillations of the equilibrium orientation, which is determined by the competition of the magnetocrystalline easy axis and the external magnetic field. An increase of the magnetic field so that $\mathrm{H_{ext}} \gg \delta\mathrm{H_a}$ leads to a suppression of the magnetic oscillations as suggested in Fig. 1(f) and observed in Fig. 2(c).

A formal description of such an acoustically driven magnetization dynamics requires us to consider free energy terms Φ_a responsible for the in-plane anisotropy. They have to comply with symmetry operations of the space group and can be written in terms of the antiferromagnetic vector [33] $\mathbf{l} = (\mathbf{M}_1 - \mathbf{M}_2)/2\mathrm{M}_0$, $\mathrm{M}_0 = |\mathbf{M}_1| = |\mathbf{M}_2|$:

$$\Phi_a = \frac{1}{2i}b(l_+^3 - l_-^3)l_z + \frac{1}{2}g(l_+^6 + l_-^6), \qquad (1)$$

where $l_\pm = l_x \pm il_y$ and b, g are cubic and hexagonal magnetic anisotropy constants, respectively, and the x axis coincides with one of the three C_2 axes. The effect of strain on the in-plane anisotropy can be phenomenologically written as a renormalization of the anisotropy constant : $b_{\mathrm{eff}} = b + \delta b(\epsilon_{ij})$ and $g_{\mathrm{eff}} = g + \delta g(\epsilon_{ij})$. Here, $\epsilon_{ij} = \epsilon_{ij}^0 + s_{ij}$ is a strain tensor consisting of a static magnetostrictive ϵ_{ij}^0 and dynamical part s_{ij}. In the linear approximation only terms proportional to ϵ_{zz} and $\epsilon_{xx} + \epsilon_{yy}$ satisfy the symmetry operations of the $FeBO_3$ space group and can contribute to Φ_a. Our experiment shows that the magnetic oscillations are caused by ϵ_{zz}. The dynamical strain-induced contributions to the effective constants of the in-plane anisotropy can be written as $\delta b_{\mathrm{dyn}} = G_4 s_{zz}$ and $\delta g_{\mathrm{dyn}} = G_6 s_{zz}$. The laser-induced dynamical strain acts like a driving force for the magnetization dynamics. Although detailed theoretical treatment of the problem will be considered elsewhere, here we note that it is based on the condition $f \ll f_{\mathrm{FMR}}$. As done in Ref. [22], minimizing the thermodynamical potential, which accounts for magnetic, elastic, and magnetoelastic energies, with respect to the antiferromagnetic vector $\mathbf{l}$, one can find the equilibrium orientation of $\mathbf{l}$. It can be shown that due to magnetoelastic terms given by Eq. (1), longitudinal strain leads to anharmonic oscillations of the spins. This theoretical framework and the field dependence of the observed 1st and 2nd harmonics of magnetic excitations allowed us to estimate the phenomenological parameters ($G_4 \sim 10^7$ erg/cm^3, $G_6 \sim 10^4$ erg/cm^3) and the laser-induced strain amplitude ($s_{zz}^0 \sim 10^{-4}$) . The fit of the experimental data with these parameters describes the experiment well [see Fig. 2(c)]. Note that static magnetostrictive deformation ϵ_{zz}^0 in $FeBO_3$ is about 10^{-5} [34], and, thus, $s_{zz}^0 \gg \epsilon_{zz}^0$. Such an inequality is the reason for the strongly anharmonic behavior of the acoustically driven oscillations of spins.

To conclude, as the observed lattice-driven dynamics can last up to few μs [35,36], it can be employed for coherent control of magnetism [37,38]. Note that the observed amplitudes of the magnetoacoustic excitation are just by a factor of 2 smaller than those required for the switching [16]. However, achieving higher magnetization deviation amplitudes is hampered by the anharmonicity of the magnetoacoustic excitation.

The authors thank B. A. Ivanov, T. Tudorovskiy, A. van Rooij, T. Toonen, and A. van Etteger for fruitful discussions and technical support. This work was supported by The Netherlands Organization for Scientific Research (NWO), the Foundation for Fundamental Research on Matter (FOM), the European Unions Seventh Framework Program (FP7/2007-2013) Grants No. NMP3-LA-2010-246102 (IFOX), No. 280555 (Go-Fast), No. 214810 (FANTOMAS), and No. 257280 (Femtomagnetism) as well as the Russian Ministry of Education and Science (14.B37.21.0899).

*d.afanasiev@science.ru.nl

[1] A. Kirilyuk, A. V. Kimel, and Th. Rasing, Rev. Mod. Phys. **82**, 2731 (2010).

[2] J. Stöhr and H. Siegmann, *Magnetism: From Fundamentals to Nanoscale Dynamics* (Springer, Berlin, 2006).

[3] I. Zutic, J. Fabian, and S. Das Sarma, Rev. Mod. Phys. **76**, 323 (2004).
[4] V. V. Kruglyak, S. O. Demokritov, and D. Grundler, J. Phys. D **43**, 260301 (2010).
[5] E. Beaurepaire, J. C. Merle, A. Daunois, and J. Y. Bigot, Phys. Rev. Lett. **76**, 4250 (1996).
[6] J. Wang, C. Sun, J. Kono, A. Oiwa, H. Munekata, L. Cywin'ski, and L. J. Sham, Phys. Rev. Lett. **95**, 167401 (2005).
[7] C. D. Stanciu, F. Hansteen, A. Kimel, A. Kirilyuk, A. Tsukamoto, A. Itoh, and Th. Rasing, Phys. Rev. Lett. **99**, 047601 (2007).
[8] K. Vahaplar, A. Kalashnikova, A. Kimel, D. Hinzke, U. Nowak, R. Chantrell, A. Tsukamoto, A. Itoh, A. Kirilyuk, and Th. Rasing, Phys. Rev. Lett. **103**, 117201 (2009).
[9] A. V. Kimel, A. Kirilyuk, P. A. Usachev, R. V. Pisarev, A. M. Balbashov, and Th. Rasing, Nature (London) **435**, 655 (2005).
[10] F. Hansteen, A. V. Kimel, A. Kirilyuk, and Th. Rasing, Phys. Rev. Lett. **95**, 047402 (2005).
[11] T. Kampfrath, A. Sell, G. Klatt, A. Pashkin, S. Mährlein, T. Dekorsy, M. Wolf, M. Fiebig, A. Leitenstorfer, and R. Huber, Nat. Photonics **5**, 31 (2010).
[12] J. W. Kim, M. Vomir, and J.-Y. Bigot, Phys. Rev. Lett. **109**, 166601 (2012).
[13] J. V. Jäger *et al.*, Appl. Phys. Lett. **103**, 032409 (2013).
[14] A. Melnikov, I. Radu, U. Bovensiepen, O. Krupin, K. Starke, E. Matthias, and M. Wolf., Phys. Rev. Lett. **91**, 227403 (2003).
[15] A. V. Scherbakov, A. S. Salasyuk, A. V. Akimov, X. Liu, M. Bombeck, C. Brüggemann, D. R. Yakovlev, V. F. Sapega, J. K. Furdyna, and M. Bayer, Phys. Rev. Lett. **105**, 117204 (2010).
[16] O. Kovalenko, T. Pezeril, and V. V. Temnov, Phys. Rev. Lett. **110**, 266602 (2013).
[17] A. J. Kurtzig, R. Wolfe, R. C. LeCraw, and J. W. Nielsen, Appl. Phys. Lett. **14**, 350 (1969).
[18] M. H. Seavey, Solid State Commun. **12**, 49 (1973).
[19] B. Yu. Sokolov, Phys. Solid State **47**, 1707 (2005).
[20] D. E. Lacklison, J. Chadwick, and J. L. Page, J. Phys. D **5**, 810 (1972).
[21] M. Borovets, A. A. Garmonov, S. G. Rudov, and Yu. M. Fedorov, JETP Lett. **50**, 466 (1989).
[22] M. B. Strugatsky and K. M. Skibinsky, Phys. Solid State **52**, 1204 (2010).
[23] A. M. Kalashnikova, A. Kimel, R. Pisarev, V. Gridnev, A. Kirilyuk, and Th. Rasing, Phys. Rev. Lett. **99**, 167205 (2007).
[24] W. Jantz, W. Wettling, and J. R. Sandercock, J. Phys. C **9**, 2229 (1976).
[25] F. Hudert, A. Bruchhausen, D. Issenmann, O. Schecker, R. Waitz, A. Erbe, E. Scheer, T. Dekorsy, A. Mlayah, and J.-R. Huntzinger, Phys. Rev. B **79**, 201307(R) (2009).
[26] Y. R. Shen, Phys. Lett. **20**, 378 (1966).
[27] E. A. Turov and V. G. Shavrov, Sov. Phys. Usp. **26**, 593 (1983).
[28] Y. R. Shen, *The Principles of Nonlinear Optics*, (John Wiley and Sons, New York, 1984).
[29] Y. Yan and K. A. Nelson, J. Chem. Phys. **87**, 6240 (1987).
[30] A. Kobyakov, M. Sauer, and D. Chowdhury, Adv. Opt. Photonics **2**, 1 (2010).
[31] M. B. Strugatsky and K. M. Skibinsky, Phys. Solid State **51**, 1172 (2009).
[32] D. Sander, Rep. Prog. Phys. **62**, 809 (1999).
[33] E. A. Turov, *Symmetry And Physical Properties Of Antiferromagnetics* (Cambridge International Science Publishing, Cambridge, England, 2010).
[34] Yu. N. Mitsay, K. M. Skibinsky, M. B. Strugatsky, A. P. Korolyuk, V. V. Tarakanov, and V. I. Khizhnyi, J. Magn. Magn. Mater. **219**, 340 (2000).
[35] B. Ya. Kotyuzhanskii and L. A. Prozorova, JETP Lett. **35**, 244 (1982).
[36] L. E. Svistov, V. L. Safonov, J. Löw, and H. Benner, J. Phys. Condens. Matter **6**, 8051 (1994).
[37] E. Rozkotová, P. Němec, N. Tesařová, P. Malý, V. Novák, K. Olejník, M. Cukr, and T. Jungwirth, Appl. Phys. Lett. **93**, 232505 (2008).
[38] E. Carpene, C. Piovera, C. Dallera, E. Mancini, and E. Puppin, Phys. Rev. B **84**, 134425 (2011).